

COMPUTER-ASSISTED SHAPE CLASSIFICATION OF MIDDLE CEREBRAL ARTERY ANEURYSMS FOR SURGICAL PLANNING

Derek Burrows, Chad Washington, Ralph Dacey, Tao Ju

Washington University in St. Louis

ABSTRACT

We present a method for classifying the shape of middle cerebral artery (MCA) aneurysms using segmented surfaces from angiograms. The classification follows a set of visual criteria established by experienced surgeons to group aneurysms based on the clipping strategies used in surgery. Starting from a centerline representation of the input, our method automatically classifies the input into one of 4 types using a combination of graph analysis and supervised learning. When evaluated on a cohort of 84 subjects, our method achieves between 60% to 69% expected classification accuracy ($p < 10^{-3}$) with zero to a moderate amount of input from novice users.

1. INTRODUCTION

Middle cerebral artery (MCA) aneurysms comprise 20-25% of all cerebral aneurysms, which are blood filled sacks in the brain arising from a weakness in the blood vessel wall. The treatment of MCA aneurysms typically involves the application of one or more clips, of varying types, at the base of the aneurysm to restore normal blood flow and alleviate the risk of rupture (see Figure 1). The choice and application of clips depends highly on the shape of the aneurysm and its spatial configuration with respect to the nearby blood vessels.

Recently, several surgeons proposed visual criteria to classify MCA aneurysms into a few types so that aneurysms of the same type can be treated with a similar clipping strategy [1, 2, 3]. Such classifications not only help surgeons with treatment planning but are also valuable for training young surgeons. However, the interpretation of these visual criteria may differ among experts, and even more so between people with different levels of training and experience. Our long-term goal is to automate the classification process so as to maximize objectivity and repeatability. The automation may eventually lead to the ability to automatically suggest clipping strategies.

As an initial step towards our goal, this paper demonstrates that the use of shape analysis and machine learning techniques can achieve a reasonable accuracy of classification when compared with expert users. We consider a set of classification rules found in a recent work [3] (see details in Section 2). We anticipate that our framework can be extended to work with other classification systems as well. The input of our method is a segmented surface capturing the region of the vessel junction that contains the aneurysm. Using a centerline representation, our method automatically labels the structural components (e.g., main and secondary branches, and the aneurysm) and extracts the geometric features that are

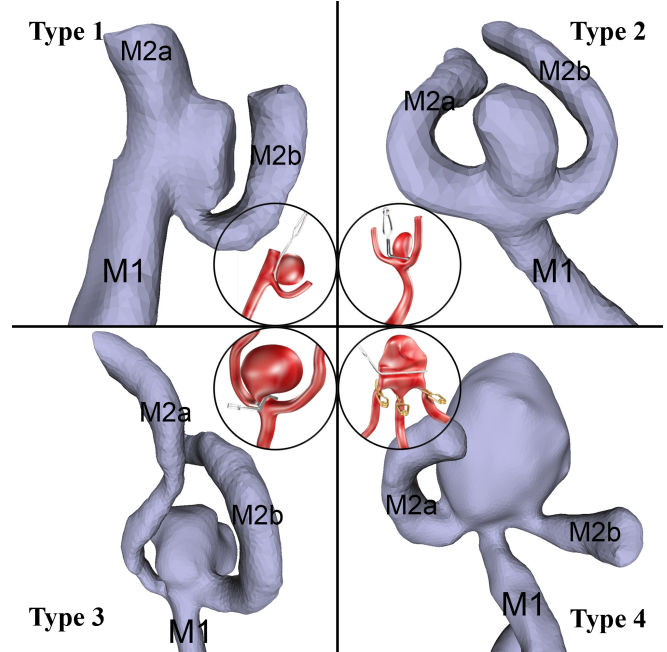


Fig. 1: Types of MCA aneurysms and illustration of their clipping strategies. Clipping strategies from: Washington, C. et al. (2013).

essential for classification (e.g., radii of the branches and the aneurysm, and the angles between them). A multi-class Support Vector Machine (SVM) based on these features is trained using 84 subjects that have already been classified by an expert. Our method achieves between 60% to 69% expected classification accuracy ($p < 10^{-3}$) with zero to a moderate amount of input from a user with no training in neurosurgery.

To our best knowledge, this is the first computational work on classifying the shape of aneurysms for surgical planning. While there is a rich literature on computer-assisted detection and segmentation of aneurysms from images, works that address the shape of aneurysms are scarce [4, 5, 6]. These works mostly offer means for describing the geometry of the aneurysm, including its volume, surface area, and differential surface properties, often in the context of assessing risk of rupture. On the other hand, we are more concerned with the spatial relationships between the aneurysm and the surrounding structures, which is crucial for selecting clipping strategies. Centerlines have been commonly used for analysis of vascular systems [7]. Our novelty is the use of centerlines to automatically label various structural components in the

aneurysm region and to extract essential geometric features for classification.

2. BACKGROUND: ANEURYSM TYPES

We adopt the following visual criteria that classify an MCA aneurysm into one of four types (see Figure 1). These criteria were developed by experienced surgeons and, are based on the geometry of the aneurysm and its neighboring vessel branches. The rationale of these criteria and the corresponding clipping strategies for each type (shown in thumbnails in Figure 1) are detailed in a separate paper [3]. Let us denote the main (incoming) branch as M1 and the two secondary (outgoing) branches as M2A and M2B. The *direction* of a branch is the vector along the branch that points away from the junction.

Type 1: A small aneurysm hangs off either M2A or M2B. M2A and M2B have dissimilar radii, and the branch with a larger radius forms an obtuse angle with M1 while the other forms an acute angle with M1.

Type 2: An aneurysm is rooted at the junction and generally lies in the plane containing M2A and M2B. M2A and M2B have similar radii and both form obtuse angles with M1.

Type 3: Similar to Type 2, except the aneurysm lies out of the plane containing M2A and M2B.

Type 4: A big aneurysm engulfs the junction. M2A and M2B have similar radii and both form acute angles with M1.

3. METHOD

Our input is a segmented surface from an angiogram encompassing the aneurysm and the nearby vessel branches, like those shown in Figure 1. The segmentation can be produced either automatically or interactively. We used *Seg-3D* [8] to produce the input data for this paper. The surfaces need to be topologically simple without spurious handles (i.e. having genus zero).

To perform classification following the visual criteria as described earlier, we need to compute shape features, including radii and directions, of both the aneurysm and the various branches. To do so, we first turn the surface model into a centerline representation using a robust thinning algorithm [9]. The algorithm produces a discrete centerline graph, made up of vertices and segments, where each vertex is equipped two metrics: a *thickness* measure that describes the radius of the largest sphere centered at the vertex that fits inside the surface, and an *elongation* measure that captures the length of the longest tube centered at the vertex that fits inside the surface. Examples of these two metrics are shown in Figure 2 (b).

The centerline graph is then used to extract the relevant shape features in three stages (detailed below). First, we label the parts of the centerline graph that correspond to the aneurysm and each of the three branches (M1, M2A, M2B). Next, we locate a “starting point” for each branch away from

the junction, which is important for estimating radii and directions. Finally, shape features are extracted and a supervised classifier is built through training. These stages are illustrated in Figure 2 (c,d,e). The separation of the stages allows the user to monitor the progress of the method and make corrections when needed. Corrections at an earlier stage will be automatically incorporated into the method in later stages.

3.1. Labeling branches and aneurysm

We perform graph analysis on the centerline graph to identify centerlines respectively for the aneurysm and branches M1, M2A and M2B.

We start by locating the junction of the three branches, which would be at a vertex with degree 3 in the centerline graph. Note that there may be multiple such vertices in the graph (e.g. the root of the aneurysm or root of a spurious centerline due to presence of noise). Our key observation is the vessel branches are, in most cases, much longer than the aneurysm on the segmented surface. Hence we look for, among all degree-3 vertices, the vertex where the *smallest* elongation measure associated with the vertex’s three edge-connected vertices is the *greatest*. Intuitively, such a vertex sits at the junction of the three longest tubular parts of the model. We call this vertex the *junction vertex*.

With the junction defined, the centerlines of the three branches are taken as the longest paths in the centerline graph starting from the junction vertex and following each of the three incident edges of the vertex. To differentiate the main branch M1 from the secondary branches M2A and M2B, we observe that M1 is usually thicker than either M2A or M2B. Hence we assign the path with the greatest average thickness measure over all its vertices as the centerline of M1. The other two paths are arbitrarily designated as M2A and M2B.

Finally, to identify the centerline of the aneurysm, we search along each branch for another degree-3 vertex that indicates the root of the aneurysm (where it is attached to the branches). Among all such degree-3 vertices, the *root vertex* of the aneurysm is assigned to be the one where the edge-adjacent vertex that does not lie on the branch centerline is associated with the greatest thickness measure.

3.2. Locating branch heads

Since the branches often curve and change thickness away from the junction, it is important to know how the surgeons define their “directions” and “radii” for classification. Our interaction with surgeons indicates that they usually pick the location on the branch right after it comes out of the junction to define the radius of the branch. The vector from the center of the junction to this location is considered as the direction of the branch. We call this location the *branch head*.

To automatically locate a branch head, we started by observing what location on a centerline is considered by a human operator to be where the branch first restores its normal radius after coming out of the junction. We observed that this location is usually not the first local minimum in the thickness profile along the centerline, but rather where the drop in thickness starts to decrease (Figure 3 left). As a result, we select the vertex on the centerline corresponding to the first local maximum in the second derivative of the thickness profile, which matches well with manually chosen branch head

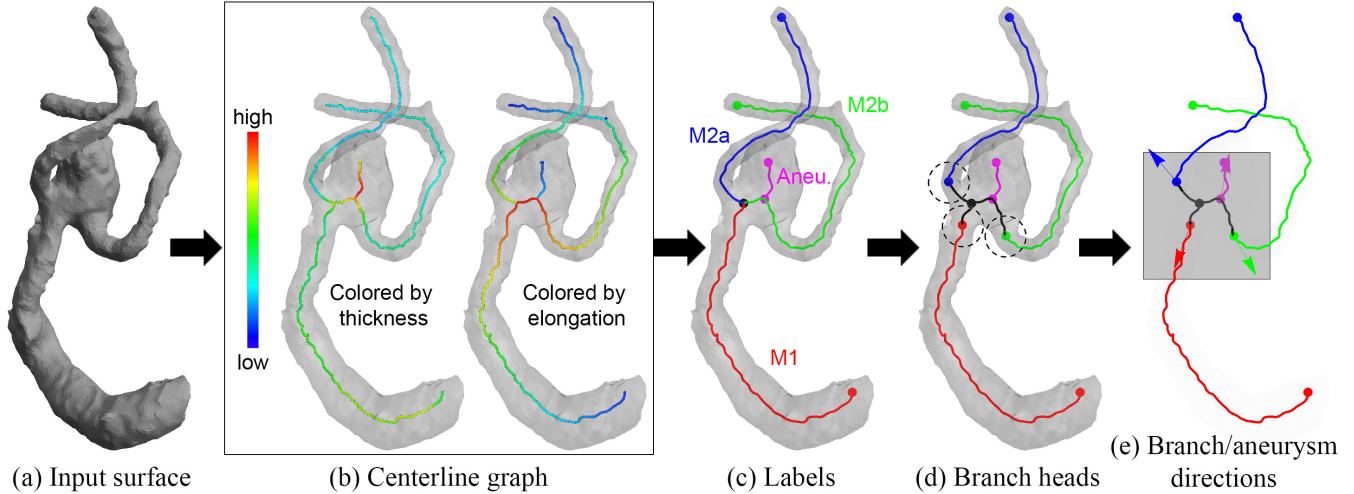


Fig. 2: The method overview: given a segmented surface (a), we first compute a centerline equipped with metrics that describe shape thickness and elongation (b), which are then used to identify the three branches and the aneurysm (c), to locate the starting points of each branch (d), and to finally extract the various radii and directions for classification (e, showing only directions).

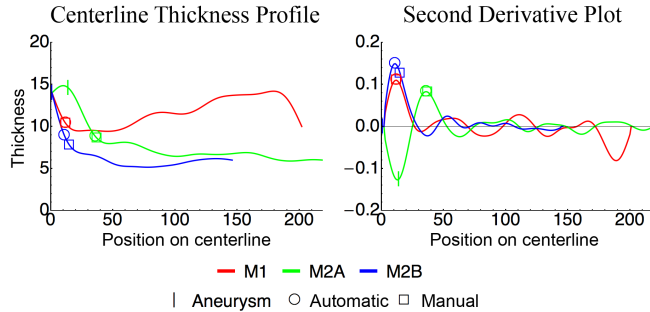


Fig. 3: Branch head locations on three centerlines of one input data, computed automatically (circles) or picked manually (squares), plotted on the thickness profile of each centerline and its secondary derivative.

locations in most of our input data (Figure 3 right). Note that for the branch where the aneurysm is rooted, the search for the branch head starts after the root vertex on the centerline.

3.3. Feature Extraction and training

For robustness, we compute the direction of a branch as a weighted average of all edge vectors on the branch’s centerline pointing from the junction vertex towards the branch head. We use a Gaussian kernel on the path distance from the branch head as the weighting function, so that centerline edges closer to the branch head have higher weights. Similarly, we compute the radius of a branch as a Gaussian-weighted average of thickness measures on all vertices over the segment of the centerline between the branch head and the end of the centerline, so that vertices closer to the branch head have higher weights. The direction and radius of the aneurysm is computed using similar weighted averaging over its own centerline.

We represent each input datum using five features, including three angles a_1, a_2, a_3 and two ratios r_1, r_2 , guided by the visual classification criteria stated earlier:

- **Branch angles:** a_1, a_2 are the angles between the direction of M1 and the direction of each of M2A and M2B. We let a_1 be the angle formed with the secondary branch with a larger radius.
- **Radii ratio:** r_1 is the ratio of the radius of the thinner secondary branch over the radius of the larger one.
- **Aneurysm-branch co-planarity:** a_3 is the angle between the aneurysm direction and the plane containing the directions of M2A and M2B.
- **Engulfment:** We approximately measure the extent to which the junction is engulfed by the aneurysm as the ratio r_2 of the size of the junction area, computed as the greatest thickness measure among all centerline edges between the junction vertex and the branch heads, and the radius of M1.

We trained a multi-class SVM (using libSVM) using a cohort of 84 subjects already labeled by an expert user into 4 classes, with 16, 36, 14, and 18 subjects in each class (see Supplementary Figure S1 for examples). SVMs are inherently sensitive to the scale of features, as well as the distribution of examples by class. We account for these sensitivities, respectively, by normalizing the set of feature vectors to zero-mean and unit-variance and then adjusting the regularization trade-off on a per-class basis to effectively weight each example by the number of examples in its class.

4. RESULTS

We evaluate the classification accuracy via two error metrics: training error and test error. The training error reports the errors in classifying the same set of data (84 subjects) that are used for training. The test error reports the average error in classifying each subject using a classifier trained on the remaining subjects (so called Leave-One-Out error). This error reflects the expected classification accuracy for never-before-seen subjects. We report errors for each class (as

Labeling	Branch Heads	Error	Type				
			1	2	3	4	All
Auto	Auto	Train	0.125	0.361	0.357	0.278	0.298
		Test	0.186	0.417	0.571	0.444	0.405
Manual	Auto	Train	0.125	0.278	0.357	0.167	0.238
		Test	0.188	0.306	0.571	0.389	0.345
Manual	Manual	Train	0.000	0.250	0.286	0.167	0.190
		Test	0.188	0.306	0.500	0.278	0.310

Table 1: Classification errors (in percentage) of our method for varying amounts of user input.

the percentage of subjects in this class that are misclassified by our method) and for all classes (as the percentage of all subjects that are misclassified). The test classification status for a small subset of training subjects can be found in Supplementary Figure S1 (a full listing can be found online at: <http://cse.wustl.edu/~taoju>).

We consider three different scenarios in which our method may be used: (1) finishing automatically without user intervention, (2) using manual inputs of labels of aneurysm and branches (replacing the algorithm in the first stage), and (3) using manual input of both labels and branch head locations (replacing the algorithm in the first and second stages). Using the centerline representation, it is fairly convenient for the user to provide these inputs. For labeling, the user only needs to click on the junction vertex, the end vertices of the three branch centerlines, the root vertex of the aneurysm, and the end vertex of the aneurysm centerline. The branch heads are picked by clicking on three more vertices on the centerline graph. Compared to shape classification of MCA aneurysm, providing these inputs (particularly the labels) requires little domain-specific training and is a much less subjective task. In our test, we found that the automated algorithm correctly labeled aneurysm and branches (matching user-provided labels) for 77% of the input.

The classification errors for each scenario are reported in Table 1. As expected, the errors drop as more user input is given. The training accuracy ranges from 71% to 81% depending on the level of user input, whereas the testing accuracy ranges from 60% to 69%. The p -values for all errors are less than 10^{-3} , indicating that they are statistically significant compared to a random classifier.

5. CONCLUSION AND DISCUSSION

We reported a computer-assisted system for classifying MCA aneurysms based on their shape for the purpose of surgical planning. We performed graph-based analysis on a centerline representation of an input (segmented) surface to achieve automatic component labeling and feature extraction. Using an off-the-shelf classifier, we achieved a minimum of 60% expected classification accuracy for never-before-seen subjects when evaluated against expert classifications, and the accuracy can be further improved with a small amount of input from users without training in the domain area.

Shape classification of aneurysms inherently involves some degree of subjectivity, even among domain experts. This is further exacerbated by the presence of ambiguous aneurysms that exhibit characteristics of multiple classes. As the next step, we would like to investigate the variance among different surgeons in applying the same set of visual classification criteria. The investigation will help us build

a better classifier, for example, by including fuzzy labels in our training data for those subjects upon which the surgeons disagreed. Furthermore, we would like to compare variability of expert classifications to the variability of classifications by less experienced users (e.g. young surgeons in training) who use our tool with different levels of manual inputs. It is our hope that, with our method, novice users will be able to achieve similar classification accuracy as experts but with less variability.

6. ACKNOWLEDGEMENTS

This work is supported in part by NSF grant IIS-1319573.

7. REFERENCES

- [1] M. V. K. Kumar, K. L. Karagiozov, L. Chen, S. Imizu, M. Yoneda, T. Watabe, Y. Kato, H. Sano, and T. Kanno, "A classification of unruptured middle cerebral artery bifurcation aneurysms that can help in choice of clipping technique.," *Minim Invasive Neurosurg*, vol. 50, pp. 132–139, 2007.
- [2] M.T. Lawton, *Seven aneurysms: Tenets and techniques for clipping*, New York: Thieme, 2010.
- [3] Chad W Washington, Tao Ju, Gregory J Zipfel, and Ralph G Dacey Jr, "Middle cerebral artery bifurcation aneurysms: An anatomical classification scheme for planning optimal surgical strategies.," *Neurosurgery*, 2013.
- [4] Robert A. McLaughlin and J. Alison Noble, "Demarcation of aneurysms using the seed and cull algorithm," in *MICCAI*, 2002, pp. 419–426.
- [5] Christof Karmonik, Anil Arat, Goetz Benndorf, Sergin Akpek, Richard Klucznik, Michel E Mawad, and Charles M Strother, "A technique for improved quantitative characterization of intracranial aneurysms.," *AJNR. American journal of neuroradiology*, vol. 25, no. 7, pp. 1158–61, Aug. 2004.
- [6] Baoshun Ma, Robert E Harbaugh, and Madhavan L Raghavan, "Three-dimensional geometrical characterization of cerebral aneurysms.," *Annals of biomedical engineering*, vol. 32, no. 2, pp. 264–73, Feb. 2004.
- [7] Marina Piccinelli, Alessandro Veneziani, David A. Steinman, Andrea Remuzzi, and Luca Antiga, "A framework for geometric analysis of vascular structures: Application to cerebral aneurysms," *IEEE Trans. Med. Imaging*, vol. 28, no. 8, pp. 1141–1155, 2009.
- [8] CIBC, "2013, Seg3D: Volumetric Image Segmentation and Visualization. Scientific Computing and Imaging Institute (SCI), Download from: <http://www.seg3d.org>.
- [9] L. Liu, E. W. Chambers, D. Letscher, and T. Ju, "A simple and robust thinning algorithm on cell complexes," *Computer Graphics Forum*, vol. 29, no. 7, pp. 2253–2260, Sept. 2010.

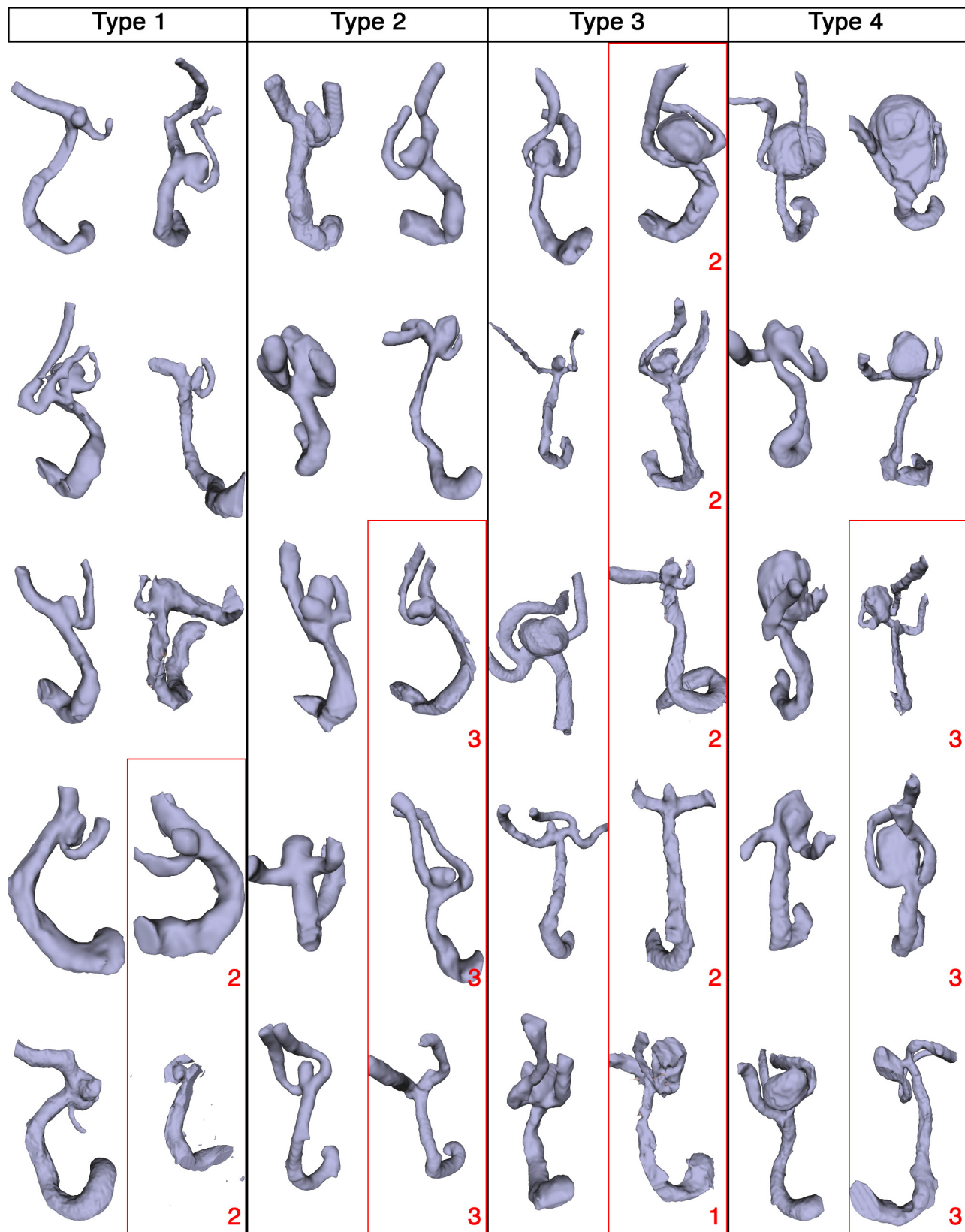


Fig. S1: Test classification status (calculated using Leave-One-Out) of a subset of aneurysm examples used for SVM training. Correctly classified examples are shown as-is, while those incorrectly classified are outlined in red and annotated with the type predicted by our algorithm. For all training examples and their classification status please visit: <http://cse.wustl.edu/~taoju>.